Proteasome activity regulates CD8+ T lymphocyte metabolism and fate specification

Christella E. Widjaja,[1] Jocelyn G. Olvera,[1] Patrick J. Metz,[1] Anthony T. Phan,[2] Jeffrey N. Savas,[3] Gerjan de Bruin,[4] Yves Leestemaker,[5,6] Celia R. Berkers,[7] Annemieke de Jong,[5] Bogdan I. Florea,[4] Kathleen Fisch,[8] Justine Lopez,[1] Stephanie H. Kim,[1] Daniel A. Garcia,[1] Stephen Searles,[9] Jack D. Bui,[9] Aaron N. Chang,[8] John R. Yates III,[3] Ananda W. Goldrath,[2] Hermen S. Overkleeft,[4] Huib Ovaa,[5,6] and John T. Chang[1]

[1]Department of Medicine and [2]Division of Biological Sciences, UCSD, La Jolla, California, USA. [3]Department of Chemical Physiology, The Scripps Research Institute, La Jolla, California, USA. [4]Leiden Institute of Chemistry, Leiden University, Leiden, The Netherlands. [5]Division of Cell Biology II, The Netherlands Cancer Institute, Amsterdam, The Netherlands. [6]Department of Chemical Immunology, Leiden University Medical Center, Leiden, The Netherlands. [7]Biomolecular Mass Spectrometry and Proteomics, Utrecht University, Utrecht, The Netherlands. [8]Center for Computational Biology and Bioinformatics, Department of Medicine, and [9]Department of Pathology, UCSD, La Jolla, California, USA.

During an immune response, CD8+ T lymphocytes can undergo asymmetric division, giving rise to daughter cells that exhibit distinct tendencies to adopt terminal effector and memory cell fates. Here we show that "pre-effector" and "pre-memory" cells resulting from the first CD8+ T cell division in vivo exhibited low and high rates of endogenous proteasome activity, respectively. Pharmacologic reduction of proteasome activity in CD8+ T cells early during differentiation resulted in acquisition of terminal effector cell characteristics, whereas enhancement of proteasome activity conferred attributes of memory lymphocytes. Transcriptomic and proteomic analyses revealed that modulating proteasome activity in CD8+ T cells affected cellular metabolism. These metabolic changes were mediated, in part, through differential expression of Myc, a transcription factor that controls glycolysis and metabolic reprogramming. Taken together, these results demonstrate that proteasome activity is an important regulator of CD8+ T cell fate and raise the possibility that increasing proteasome activity may be a useful therapeutic strategy to enhance the generation of memory lymphocytes.

Introduction

In response to microbial infection, CD8+ T lymphocytes undergo rapid clonal proliferation associated with differentiation into terminal effector and memory cell subsets. Terminally differentiated, short-lived effector cells produce inflammatory cytokines, such as IFN-γ and TNF-α, and release cytolytic granules to kill infected cells. Memory CD8+ T cells are capable of stem cell–like self-renewal, and certain subsets of memory cells, such as central memory T cells (T_{CM} cells), can proliferate rapidly in response to recurrent infections. Specification of these CD8+ T cell subsets is driven by diverse factors, including TCR signal strength, costimulatory molecules, cytokine signals, transcription factors, and the microenvironment (1–4).

Prior studies have shown that a single naive CD8+ T cell can give rise to both terminal effector and memory lymphocytes (5–7). One mechanism by which terminal effector and memory cells can be derived from a single naive cell is asymmetric cell division, an evolutionarily conserved process in which cellular components are unequally localized to opposing poles of a mitotic cell, thereby resulting in daughter cells with tendencies toward distinct fates from their inception (8, 9). T-bet, a transcription factor critical in terminal effector CD8+ T lymphocyte differentiation (10), has been demonstrated to undergo asymmetric localization during the first cell division (11). T-bet asymmetry during mitosis has been shown to be mediated by localized degradation due to asymmetric segregation of the proteasome machinery in dividing CD8+ T cells (11). This observation raised the possibility that the degree of proteasome activity experienced by daughter CD8+ T cells emerging from the first division in vivo in response to microbial infection may play a role in regulating the eventual fate of these cells.

The 26S proteasome is a multi-subunit protein complex that performs the majority of cellular protein degradation in a highly regulated manner. It comprises a 20S core particle that contains catalytic subunits and 19S regulatory particles, which attach directly to the outer rings of the core particle to regulate substrate unfolding and entry. Lymphocytes can also express specialized inducible immunoproteasome subunits, which have been shown to play a role in antigen processing and the generation of a diverse T cell repertoire (12, 13). Proteins are marked for degradation by the post-translational process of ubiquitination, which is also reversible (14–17). Thus, ubiquitination and deubiquitination of proteins, as well as the level of proteasome activity itself, can control the rate of protein degradation.

Regulation of endogenous proteasome activity has been previously shown to control cell fate decisions of human embryonic stem cells (18, 19) and cancer stem cells (20, 21). Moreover, recent studies in lymphocytes have shown that proteasome activity can also influence their differentiation and function (22–26). These findings, along with the observation of asymmetric proteasome

Conflict of interest: The authors have declared that no conflict of interest exists.
Submitted: September 26, 2016; **Accepted:** July 14, 2017.
Reference information: *J Clin Invest*. 2017;127(10):3609–3623.
https://doi.org/10.1172/JCI90895.

segregation within mitotic CD8$^+$ T cells (11), led us to hypothesize that proteasome activity may be an important regulator of CD8$^+$ T lymphocyte fate specification.

Here we show that "pre-effector" and "pre-memory" daughter cells emerging from the first CD8$^+$ T cell division in vivo exhibited low and high rates of proteasome activity, respectively. Pharmacologic alteration of proteasome activity resulted in changes to CD8$^+$ T cell effector and memory differentiation. Proteasome-mediated effects on CD8$^+$ T cell differentiation were due, in part, to effects on Myc, a transcription factor that controls glycolysis and metabolic reprogramming. Together, these results suggest that proteasome activity regulates CD8$^+$ T lymphocyte metabolism and fate specification and suggest the possibility that increasing proteasome activity may be a useful therapeutic strategy to enhance the generation of memory lymphocytes.

Results

CD8$^+$ T cells with unique fate tendencies exhibit distinct levels of proteasome activity. It has been previously shown that CD8$^+$ T lymphocytes can asymmetrically segregate certain cellular components, including the proteasome machinery, during their first division in response to microbial infection (11). We therefore asked whether asymmetric localization of the proteasome during mitosis might lead to distinct proteasome activity levels in the nascent daughter cells following division. Using a model system that we have previously employed to examine T cells undergoing their first division in vivo in response to microbial infection (9), we assessed the total activity of the proteasome catalytic subunits using irreversible, covalent activity–based probes that have been previously described (Supplemental Figure 1; supplemental material available online with this article; https://doi.org/10.1172/JCI90895DS1) (21, 27, 28).

OT-I CD8$^+$ T cells, which have transgenic expression of the T cell antigen receptor that recognizes a specific OVA epitope, were labeled with a fluorescent dye (CFSE) that enables tracking of cell division. Cells were then adoptively transferred into recipient mice that were infected 24 hours later with *Listeria monocytogenes*–expressing OVA (Lm-OVA). At 45 hours after infection, mice were sacrificed and splenocytes analyzed by flow cytometry. Asymmetric CD8$^+$ T cell division has been shown to yield one daughter cell (phenotypically CD8^{hi}IL-2Rα^{hi}CD62L^{lo}) exhibiting a predisposition toward the terminal effector fate ("pre-effector") and another daughter cell (phenotypically CD8^{lo}IL-2Rα^{lo}CD62L^{hi}) exhibiting a predisposition toward the long-lived memory fate ("pre-memory") (29). We observed that pre-effector first-division cells exhibited lower proteasome activity, compared with pre-memory first-division cells (Figure 1A). Moreover, CD8$^+$ T cells exhibiting low proteasome activity expressed higher levels of effector lymphocyte–associated molecules (granzyme B [*Gzmb*], T-bet [*Tbx21*]) and lower levels of memory lymphocyte–associated molecules (Bcl-2, IL-7Rα, Tcf7) compared with their counterparts exhibiting low proteasome activity (Figure 1, B and C). Notably, these patterns of proteasome activity observed in early differentiating cells that had undergone their first division were distinct from those of mature, fully differentiated T lymphocytes. KLRG1^{hi}IL-7Rα^{lo} terminal effector cells exhibited proteasome activity similar to that of naive (CD62L^{hi}CD44^{lo}) CD8$^+$ T cells, whereas effector memory (CD44^{hi}CD62L^{lo}) and central memory lymphocytes (CD44^{hi}CD62L^{hi}), assessed at 60 days after infection, exhibited lower proteasome activity compared with naive cells (Figure 1D). Taken together, these findings suggest the possibility that the eventual fates of CD8$^+$ T lymphocytes that have undergone their first asymmetric division in vivo in response to microbial infection might be influenced by their levels of proteasome activity.

Proteasome activity in activated CD8$^+$ T cells influences their fate and function. We next sought to determine whether the predisposition of first-division pre-effector and pre-memory CD8$^+$ T cells toward different fates might be mechanistically related to their distinct levels of proteasome activity. We reasoned that treating cells with a pharmacologic inhibitor or activator would enable us to recapitulate the low and high levels of intrinsic proteasome activity exhibited in vivo after the first cell division (Figure 1A). We first established that proteasome activity could be modulated in CD8$^+$ T cells with the pan-subunit proteasome inhibitor epoxomicin (Figure 2A). We then screened a panel of proteasome activators that has been shown to increase proteasome activity in immortalized cell lines (30). Several of these compounds also increased proteasome activity in CD8$^+$ T cells (Figure 2A).

Next, we evaluated whether modulation of proteasome activity could influence effector and memory lymphocyte differentiation using a previously described in vitro differentiation system (31). CD8$^+$ T cells were stimulated with their cognate peptide for 48 hours, followed by culture with either IL-2 or IL-15 along with proteasome inhibitor, proteasome activator, or vehicle control. In response to IL-2, vehicle-treated cells were able to differentiate into "effector-like" lymphocytes characterized by high expression of IL-2Rα. Relative to vehicle-treated cells, reducing proteasome activity in IL-2 culture conditions increased the proportion of IL-2Rα^{hi} effector-like lymphocytes, whereas increasing proteasome activity reduced the proportion of these cells (Figure 2B, top row). In response to IL-15, vehicle-treated cells differentiated into "memory-like" lymphocytes characterized by high expression of CD62L. Reducing proteasome activity in IL-15 culture conditions reduced the proportion of CD62L^{hi} memory-phenotype cells, whereas increasing proteasome activity with certain proteasome activators (activators 1, 4, 5, and 9) increased the proportion of these cells (Figure 2B, bottom row).

We sought to determine whether modulation of proteasome activity might alter production of inflammatory cytokines, a measure of effector CD8$^+$ T cell function. We purified CD8$^+$ T cells and transiently treated them with proteasome inhibitor, proteasome activators, or vehicle control, followed by drug washout. Cells were then activated in vitro with plate-bound anti-CD3 and anti-CD28 antibodies; 48 hours later, we assessed the capacity of the cells to produce IFN-γ and TNF-α. We observed that cells treated with proteasome inhibitor exhibited an enhanced capacity to produce IFN-γ relative to control-treated cells (Figure 2C), while one of the proteasome activators we tested (activator 9) reduced cytokine production by CD8$^+$ T cells; we selected this proteasome activator, revealed to be cyclosporine, for subsequent experiments. The activators we tested were identified in a high-throughput screen solely based on their ability to increase proteasome activity (30); thus, they may act through different mechanisms and have unique functional properties.

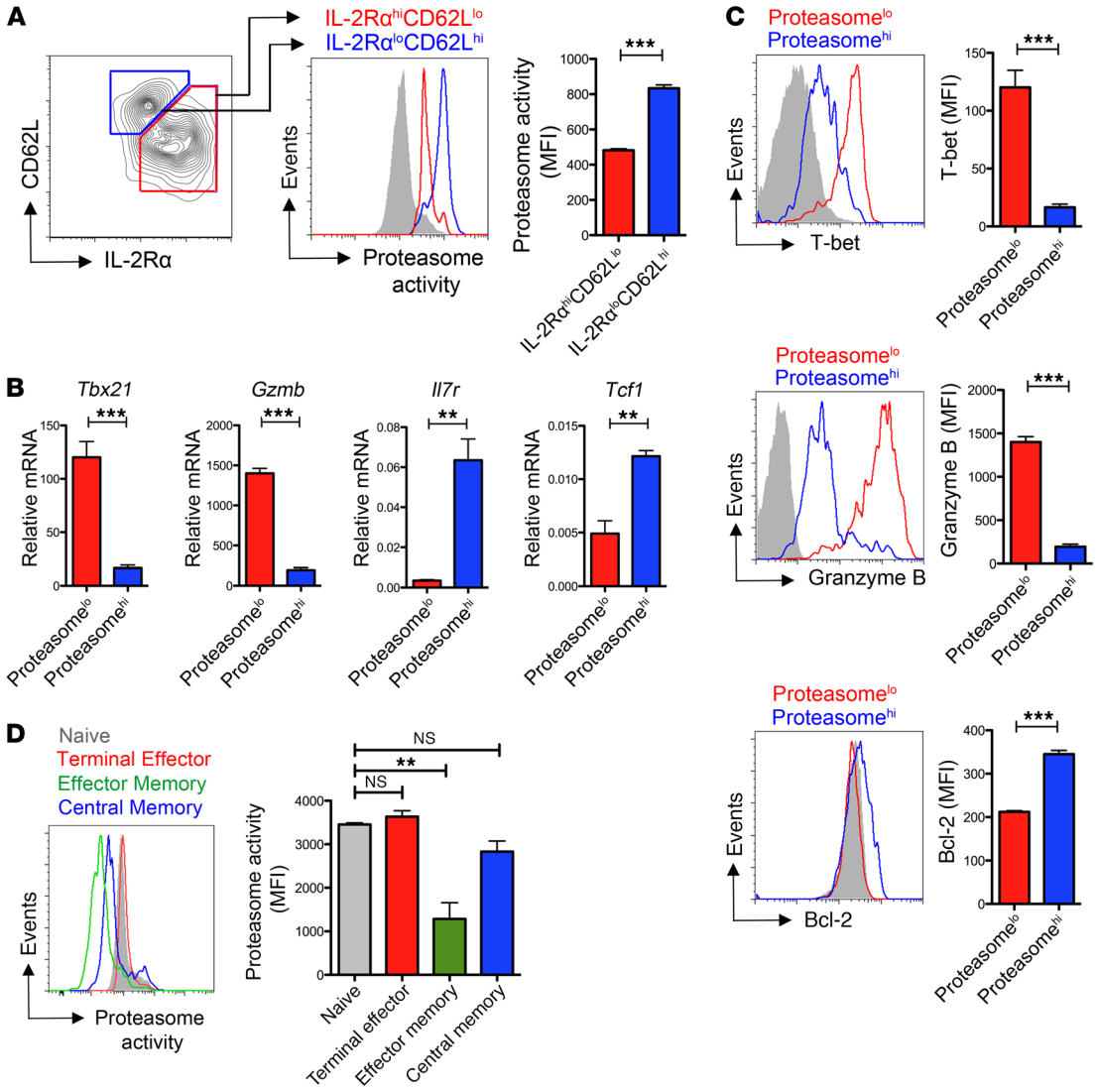

Figure 1. Differentially fated CD8⁺ T cells exhibit distinct rates of endogenous proteasome activity. (**A**) Proteasome activity, assessed by flow cytometry, of gated first division (second CFSE peak) of putative pre-effector IL-2Rα^{hi}CD62L^{lo} and pre-memory IL-2Rα^{lo}CD62L^{hi} OT-I CFSE-labeled CD8⁺ T cells adoptively transferred into recipient mice subsequently infected with Lm-OVA and analyzed 45 hours after infection. (**B**) Expression of *Tbx21*, *Gzmb*, *Il7r*, and *Tcf1* mRNA in FACS-sorted first-division proteasome activity^{lo}IL-2Rα^{hi}CD62L^{lo} (red bars) and proteasome activity^{hi}IL-2Rα^{lo}CD62L^{hi} (blue bars) cells. Expression is normalized to the average of *Rpl13* and *Rn18s* mRNA. (**C**) Flow cytometry analysis (left) and mean fluorescence intensity (MFI) of T-bet, granzyme B, and Bcl-2 in first-division proteasome activity^{lo}IL-2Rα^{hi}CD62L^{lo} (red) and proteasome activity^{hi}IL-2Rα^{lo}CD62L^{hi} (blue) cells. Gray histograms represent isotype control–stained first-division cells. (**D**) Proteasome activity, assessed by flow cytometry, of gated naive (CD8⁺CD45.1⁺CD62L^{hi}CD44^{lo} cells; uninfected mice), terminal effector (CD8⁺CD45.1⁺CD44^{hi}KLRG1^{hi}IL-7R^{lo} cells; 7 days after infection), effector memory (CD8⁺CD45.1⁺CD44^{hi}CD62L^{lo}; 60 days after infection), and central memory (CD8⁺CD45.1⁺CD44^{hi}CD62L^{hi}; 60 days after infection) adoptively transferred into CD45.2 recipient mice followed by Lm-OVA infection and analyzed 7 or 60 days after infection. Data are representative of at least 3 independent experiments (**A**, **C**, and **D**) or 3 biological replicates from 3 independent experiments (**B**) with $n \geq 4$ mice per group. Error bars represent SEM of 3 replicates. N.S., not significant ($P > 0.05$), $^{**}P < 0.01$, $^{***}P < 0.001$ (**A**–**C**, Student's 2-tailed *t* test; **D**, 1-way ANOVA with Dunnett's post-test).

Cyclosporine is an immunosuppressive drug (32) that is commonly used to treat transplant rejection; however, it was not previously known to have effects on proteasome activity. We therefore sought to distinguish the proteasome-modulating effects of cyclosporine on CD8⁺ T cell differentiation from its other known effects on the immune system. A major mechanism of action by which cyclosporine acts is binding to its cognate intracellular receptor, cyclophilin; inhibiting the calcium/calmodulin-regulated phosphatase calcineurin; and preventing nuclear translocation of the transcription factor NFAT (33, 34). Thus, to experimentally distinguish between NFAT- and proteasome-dependent effects, we asked whether transient pretreatment of CD8⁺ T cells with cyclosporine followed by drug washout prior to activation, the experimental methodology we used in Figure 2C, could prevent nuclear translocation of NFAT. In contrast to continuous treatment with cyclosporine, we observed that transient pretreatment of cells followed by drug washout prior to activation did not prevent NFAT nuclear translocation (Supplemental Figure 2, A and B). In support of these results, we also evaluated a second calcineurin inhibitor, tacrolimus, for effects on proteasome activ-

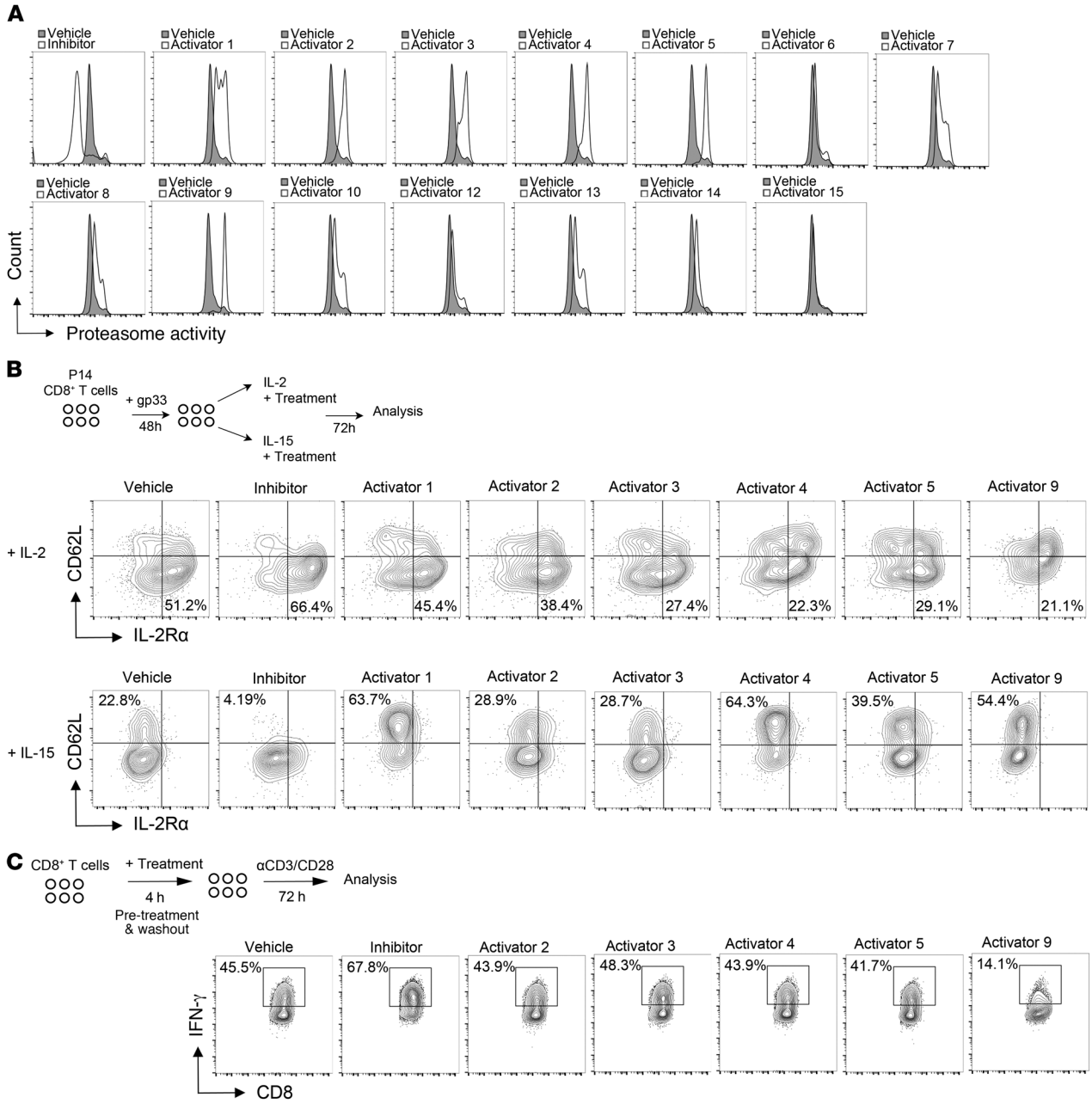

Figure 2. Level of proteasome activity influences CD8⁺ T cell differentiation in vitro. (**A**) Proteasome activity, assessed by flow cytometry, of naive CD8⁺ T cells following 4-hour culture with vehicle, proteasome inhibitor, or proteasome activators. The same vehicle control was used to compare against all experimental groups and is displayed in all histograms. (**B**) Flow cytometry analysis of in vitro IL-2Rα^{hi}CD62L^{lo} effector-like and IL-2Rα^{lo}CD62L^{hi} memory-like P14 CD8⁺ T cells. Cells were activated for 2 days with gp33–41 peptide and T cell–depleted splenocytes, then cultured in IL-2 (top row) or IL-15 (bottom row) conditions in the presence of vehicle, proteasome inhibitor, or indicated proteasome activators for an additional 3 days. (**C**) Flow cytometry analysis of intracellular IFN-γ at 72 hours after activation in CD8⁺ T cells transiently treated for 4 hours with vehicle, proteasome inhibitor, or proteasome activators followed by drug washout prior to activation with anti-CD3 and anti-CD28 antibodies. Data are representative of at least 2 independent experiments (**A**–**C**).

ity and CD8⁺ T cell differentiation. In contrast to cyclosporine, addition of tacrolimus did not increase proteasome activity in CD8⁺ T cells or promote the differentiation of memory-like cells in IL-15 conditions in vitro (Supplemental Figure 3, A and B). Taken together, these results provide evidence that the observed effects of cyclosporine on CD8⁺ T cell differentiation may be mediated by increasing proteasome activity, at least when administered transiently. We therefore proceeded to test the proteasome-mediated effects of cyclosporine, which we will refer to as "proteasome activator," in subsequent experiments.

Using an in-gel proteasome activity assay and a luminescent substrate assay, we confirmed our flow cytometry finding that proteasome activity could be reliably modulated in CD8⁺ T cells with proteasome inhibitor and activator (Figure 3, A–C). We also analyzed CD8⁺ T cells treated with proteasome inhibitor or activator and found that neither drug affected the expression of structural

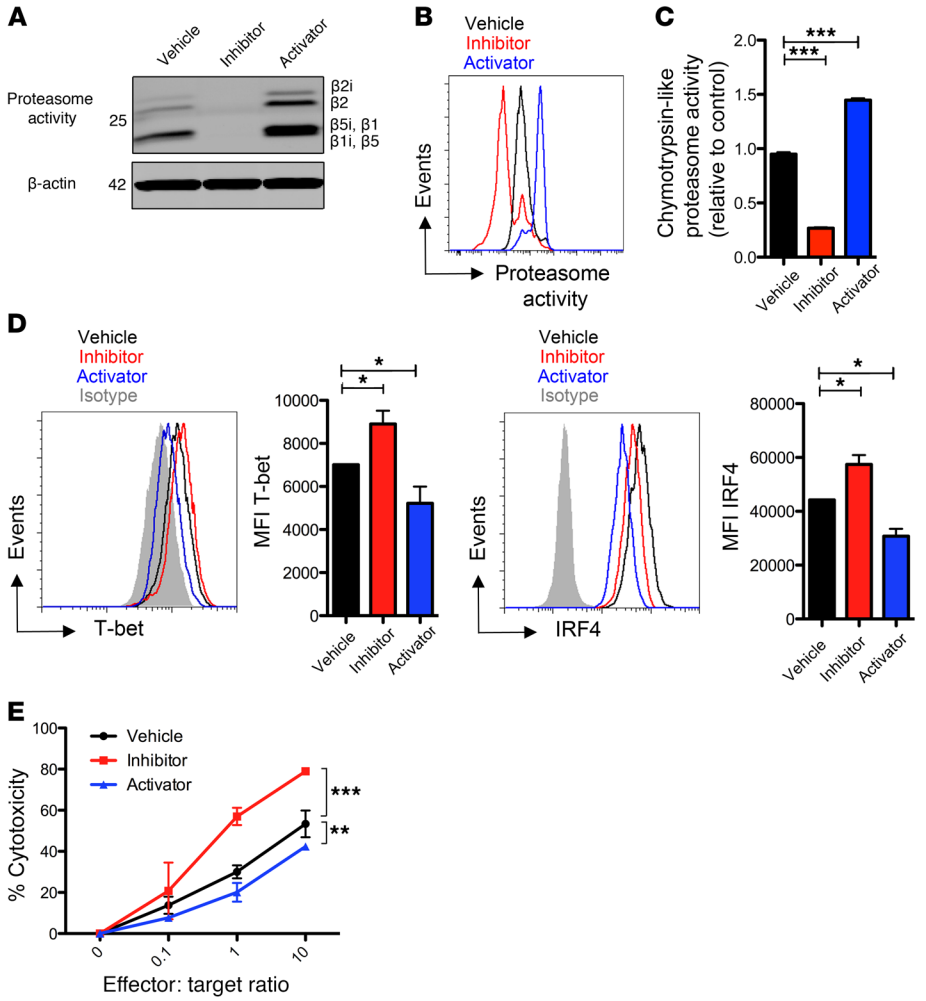

Figure 3. Modulation of proteasome activity influences CD8⁺ T cell function in vitro. (**A**) Proteasome activity, assessed by in-gel assay, of naive CD8⁺ T cells following 4 hours of culture with vehicle, proteasome inhibitor, or proteasome activator. Immunoblotting was performed with anti–β-actin antibodies to confirm equal loading of samples. (**B**) Proteasome activity, assessed by flow cytometry, of cells cultured with vehicle (black line), proteasome inhibitor (red line), or proteasome activator (blue line). (**C**) Proteasome activity, assessed by bioluminescent chymotrypsin-like proteolytic assay, of cells cultured with proteasome inhibitor (red bar) or proteasome activator (blue bar) and normalized to vehicle control (black bar). (**D**) Flow cytometry analysis (left) and MFI (right) of T-bet and IRF4 at 72 hours after activation in CD8⁺ T cells transiently treated for 4 hours with vehicle, proteasome inhibitor, or proteasome activator prior to activation with anti-CD3 and anti-CD28 antibodies. (**E**) Percent specific cytotoxicity of OT-I CD8⁺ T cells treated transiently with vehicle (black line), proteasome inhibitor (red line), or proteasome activator (blue line) prior to culture with T cell–depleted splenocytes and OVA peptide. CD8⁺ T cells were incubated with an equal ratio of peptide-pulsed and unpulsed splenocytes in varying effector cell to target cell ratios. Cytotoxicity was calculated as the difference in the percentage of live events between pulsed and unpulsed target cells, normalized to the live percentage of unpulsed target cells. Data are representative of at least 2 independent experiments (**A**–**C**) or least 3 biologic replicates from 3 independent experiments (**D** and **E**). Error bars represent SEM of 3 replicates. $*P < 0.05$, $**P < 0.01$, $***P < 0.001$ (**C** and **D**, 1-way ANOVA with Dunnett's post-test; **E**, repeated measures 1-way ANOVA).

and catalytic subunits of the 20S proteasome compared with cells treated with vehicle control (Supplemental Figure 4, A and B). We then tested whether modulation of proteasome activity might alter other attributes of effector CD8⁺ T cell differentiation and function in addition to cytokine production. Indeed, compared with control-treated cells, proteasome inhibitor–treated cells exhibited higher levels of T-bet and IRF4 (Figure 3D), key transcription factors that have been linked with terminal effector cell differentiation and function (10, 35). Finally, proteasome inhibitor–treated CD8⁺ T cells also exhibited increased cytotoxicity when incubated with peptide-pulsed target cells compared with vehicle-treated cells, whereas CD8⁺ T cells with increased proteasome activity exhibited decreased levels of cytotoxic activity (Figure 3E). Together these observations suggested that levels of proteasome activity might influence CD8⁺ T lymphocyte fate specification, at least in vitro.

We next sought to examine whether levels of proteasome activity could affect this process in vivo and utilized an experimental approach that would enable us to selectively modulate proteasome activity within early differentiating CD8⁺ T lymphocytes without affecting the cells and tissues of recipient mice. We pretreated OT-I cells with proteasome inhibitor or vehicle control followed by drug washout, adoptively transferred the cells into congenically marked recipients, then infected the recipients with Lm-OVA; donor-derived CD8⁺ T cells were then analyzed at days 7 and 50 after infection (Figure 4A). Cells that had been treated with proteasome inhibitor or vehicle control gave rise to comparable numbers of effector cells on day 7 after infection (Figure 4B). However, compared with control-treated cells, proteasome inhibitor–treated cells exhibited a significant reduction in the proportion of KLRG1^{lo}IL-7R^{hi} memory precursor cells (Figure 4C) (10) and expressed higher levels of transcription factors T-bet, Eomes, and IRF4 (Figure 4D). On day 50 after infection, compared with control-treated cells, proteasome inhibitor–treated cells gave rise to markedly fewer memory CD8⁺ T cells (Figure 4E); these cells expressed higher levels of KLRG1; lower levels of IL-7R, CD122, and CD27, molecules associated with memory cell survival (36, 37); and reduced levels of the antiapoptotic molecule Bcl-2 (Figure 4, F and G) (36, 37). Upon re-challenge, mice that had received proteasome inhibitor–treated cells exhibited significantly reduced secondary re-expansion (Figure 4H) compared with control-treated cells, supporting the hypothesis that inhibiting proteasome activity in CD8⁺ T cells results in reduced memory differentiation.

To determine whether increasing proteasome activity in CD8⁺ T cells might enhance their capacity to differentiate into memory lymphocytes, we transiently pretreated OT-I CD8⁺ T cells with

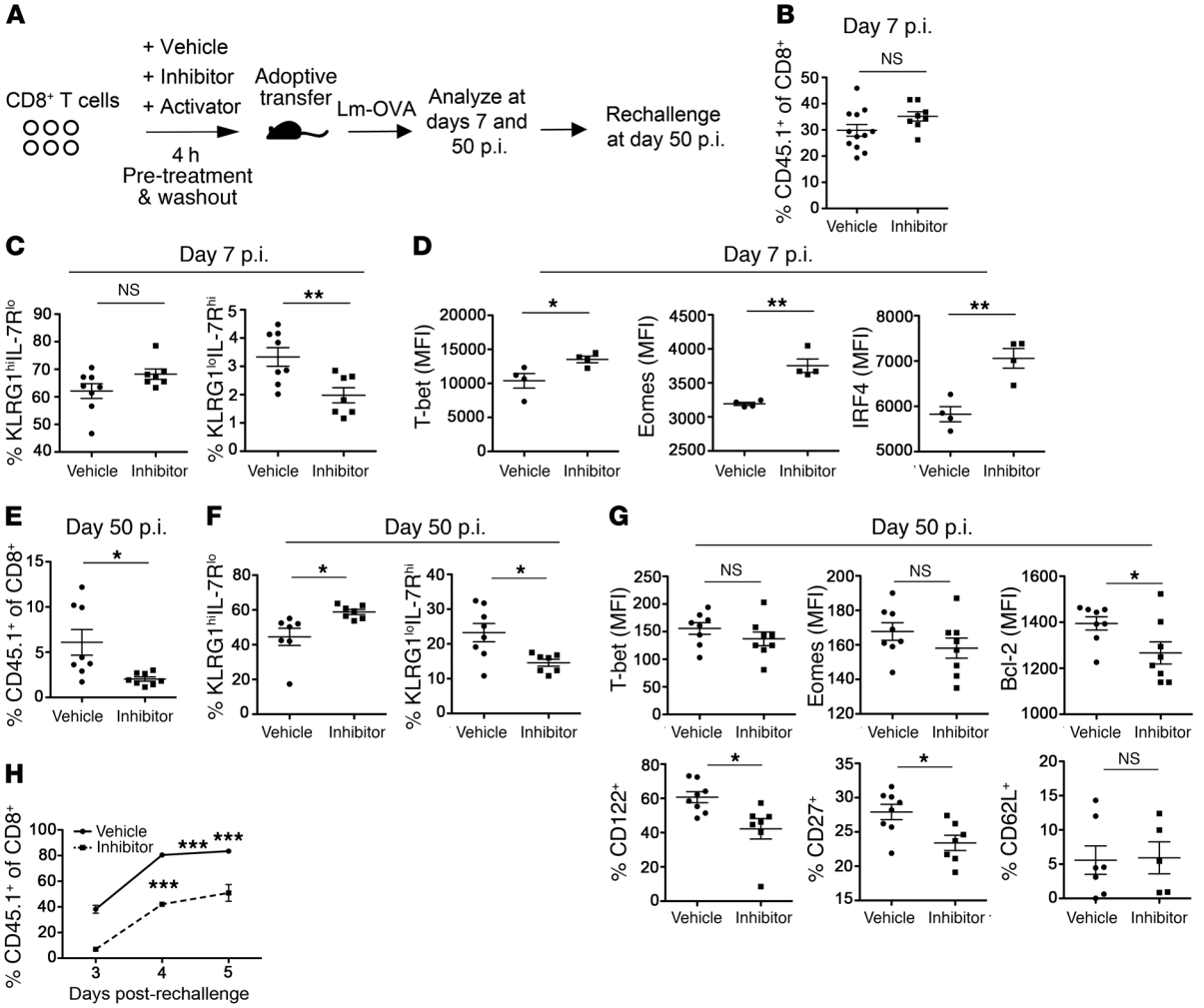

Figure 4. Proteasome inhibition reduces CD8⁺ T cell memory formation in vivo. (**A**) Experimental design. CD45.1⁺ OT-I CD8⁺ T cells were transiently treated with vehicle control, proteasome inhibitor, or proteasome activator, then adoptively transferred into CD45.2 recipients that were subsequently infected with 10^3 CFU Lm-OVA; mice were analyzed on days 7 and 50 after infection (p.i.). (**B**) Percentages of CD45.1⁺ vehicle- and proteasome inhibitor–treated CD8⁺ T cells, analyzed by flow cytometry on day 7 after infection. (**C**) Percentages of KLRG1^{hi}IL-7R^{lo} and KLRG1^{lo}IL-7R^{hi} cells, gated on CD45.1⁺CD8⁺ cells, as in **B**. (**D**) T-bet, Eomes, and IRF4 expression (MFI) within gated CD45.1⁺CD8⁺ cells, as in **B**. (**E**) Percentages of CD45.1⁺ vehicle- and proteasome inhibitor–treated CD8⁺ T cells on day 50 after infection. (**F**) Percentages of KLRG1^{hi}IL-7R^{lo} and KLRG1^{lo}IL-7R^{hi} cells, gated on CD45.1⁺CD8⁺ cells, as in **E**. (**G**) T-bet, Eomes, and Bcl-2 expression (MFI) and percentages of cells expressing CD122, CD27, or CD62L; cells were gated on CD45.1⁺CD8⁺ T cells, as in **E**. (**H**) Proliferative response of CD45.1⁺CD8⁺ T cells in response to re-infection with 10^5 CFU Lm-OVA in immune mice that had received cells treated with vehicle or proteasome inhibitor 50 days prior. (**B**–**H**) Data are representative of at least two independent experiments with $n \geq 4$ mice per group; error bars represent SEM of 3 replicates. N.S., $P > 0.05$; $^*P < 0.05$, $^{**}P < 0.01$, $^{***}P < 0.001$ (Student's t test).

proteasome activator or vehicle control followed by drug washout, adoptively transferred the cells into recipient mice, then infected the recipients with Lm-OVA. We observed that proteasome activator–treated cells expanded to the same degree as vehicle-treated cells by day 7 after infection (Figure 5A). Compared with control-treated cells, proteasome activator–treated cells tended to have a KLRG1^{lo} IL-7R^{hi} phenotype (Figure 5B), although their expression of T-bet and Eomes was comparable (Figure 5C). Although proteasome activator–treated cells gave rise to similar numbers of total memory cells on day 50 after infection compared with control cells (Figure 5D), they had decreased expression of KLRG1 and increased IL-7R, and they exhibited higher expression of Bcl-2, CD122, CD27, and CD62L, indicating that these memory cells were more likely to be T_{CM} cells (10) (Figure 5, E and F). Proteasome activator–treated cells exhibited significantly higher secondary re-expansion in response to rechallenge (Figure 5G). Taken together, these results suggest that the level of proteasome activity in CD8⁺ T cells early during their differentiation may play a critical role in regulating memory lymphocyte fate specification and function.

Last, we sought to determine whether manipulation of proteasome activity during late phases of differentiation would still affect the differentiation of effector and memory cells. CD8⁺ T cells were activated in vitro for 2 days, then cultured with IL-2 to induce effector-like differentiation or IL-15 to induce memory-like differentiation. Proteasome inhibitor or activator was added at the same time as cytokines ("early condition") or 2 days later ("late condition"). Treatment with proteasome inhibitor increased the percentage of effector-like IL-2Rα^{hi}CD62L^{lo} cells and reduced

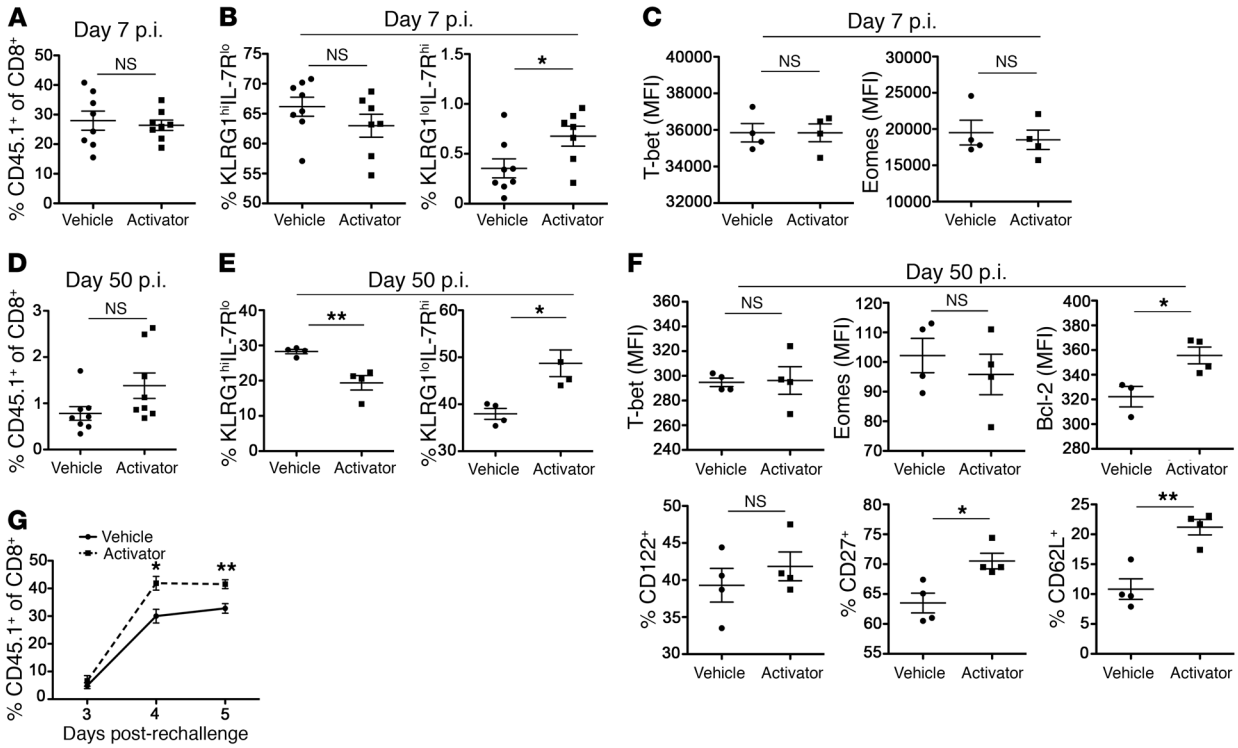

Figure 5. Proteasome activation enhances generation of central memory CD8⁺ T cells in vivo. (**A**) Percentages of CD45.1⁺ vehicle- and proteasome activator–treated CD8⁺ T cells, analyzed by flow cytometry on day 7 after infection. (**B**) Percentage of KLRG1^{hi}IL-7R^{lo} and KLRG1^{lo}IL-7R^{hi} cells, gated on CD45.1⁺ CD8⁺ cells. (**C**) T-bet and Eomes expression within gated CD45.1⁺CD8⁺ cells, as in **I**. (**D**) Percentages of CD45.1⁺ vehicle- and proteasome activator–treated CD8⁺ T cells, analyzed by flow cytometry on day 50 after infection. (**E**) Percentage of KLRG1^{hi}IL-7R^{lo} and KLRG1^{lo}IL-7R^{hi} cells, gated on CD45.1⁺ CD8⁺ cells. (**F**) T-bet, Eomes, or Bcl-2 expression (MFI) and percentages of cells expressing CD122, CD27, or CD62L; cells were gated on CD45.1⁺CD8⁺ T cells as in **L**. (**G**) Proliferative response of CD45.1⁺ CD8⁺ T cells in response to re-infection with 10^5 CFU Lm-OVA in immune mice that had received cells treated with vehicle or proteasome activator 50 days prior. (**A**–**G**) Data are representative of at least 2 independent experiments with $n \geq 4$ mice per group; error bars represent SEM of 3 replicates. N.S., $P > 0.05$; $^*P < 0.05$, $^{**}P < 0.01$ (Student's t test).

differentiation of memory-like IL-2Rα^{lo}CD62L^{hi} cells regardless of when the drug was added (Supplemental Figure 5). However, treatment with proteasome activator only increased differentiation into memory-like cells or reduced differentiation into effector-like cells when added at an early stage of differentiation (Supplemental Figure 5). These results suggest that proteasome inhibitors, but not proteasome activators, may be capable of altering CD8⁺ T cell fate specification even after cells have begun the process of differentiation.

Proteasome activity influences transcriptomic and proteomic profiles of activated CD8⁺ T cells. To begin to investigate the molecular mechanisms underlying proteasome-mediated regulation of terminal effector and memory lymphocyte differentiation, we performed microarray analysis of CD8⁺ T cells treated with proteasome inhibitor, proteasome activator, or vehicle control activated for 24 hours in vitro. 470 and 1,461 genes were significantly differentially expressed in inhibitor-treated and activator-treated CD8⁺ T cells, respectively, compared with control-treated cells (Figure 6, A and B). Proteasome activator–treated cells differentially expressed several transcripts that have been previously reported to be associated with T cell function, survival, and memory (Figure 6, B and C), including *Ifng*, *Il2*, *Tbx21*, *Eomes*, *Bcl2*, *Klf2*, and *Il7r*. By contrast, many of these genes did not differ significantly between groups receiving control treatment and those receiving proteasome inhibitor treatment (Supplemental Figure 6).

Differentially expressed genes were subjected to pathway analysis to determine relevant Gene Ontology biological processes. These analyses identified metabolic processes among the most significantly affected pathways; these processes included apoptosis, lipid metabolism, cellular protein metabolism, and cell proliferation (Figure 6, D and E). Gene set enrichment analysis (GSEA) revealed that transcripts expressed in proteasome inhibitor–treated cells were significantly enriched within the set of genes associated with effector CD8⁺ T cells obtained from the Molecular Signatures Database (MSigDB; http://software.broadinstitute.org/gsea/msigdb; Supplemental Table 1 and Figure 6F). Conversely, transcripts upregulated in proteasome activator–treated cells were significantly enriched within the set of genes associated with naive and memory CD8⁺ T cells (Figure 6F). Taken together, these data suggest that the low and high proteasome activity levels induced by proteasome inhibitor and activator resulted in differential regulation of cellular metabolic processes, which may lead to gene expression patterns resembling those found in effector and memory CD8⁺ T cells, respectively.

We next sought to identify categories of proteins that might be differentially affected by distinct levels of proteasome activity. We performed a quantitative shotgun proteomic screen using stable isotope labeling by amino acids in cell culture (SILAC), a method in which newly synthesized proteins are differentially labeled with different isotopes. CD8⁺ T cells were treated with proteasome inhibitor, proteasome activator, or vehicle control and activated in

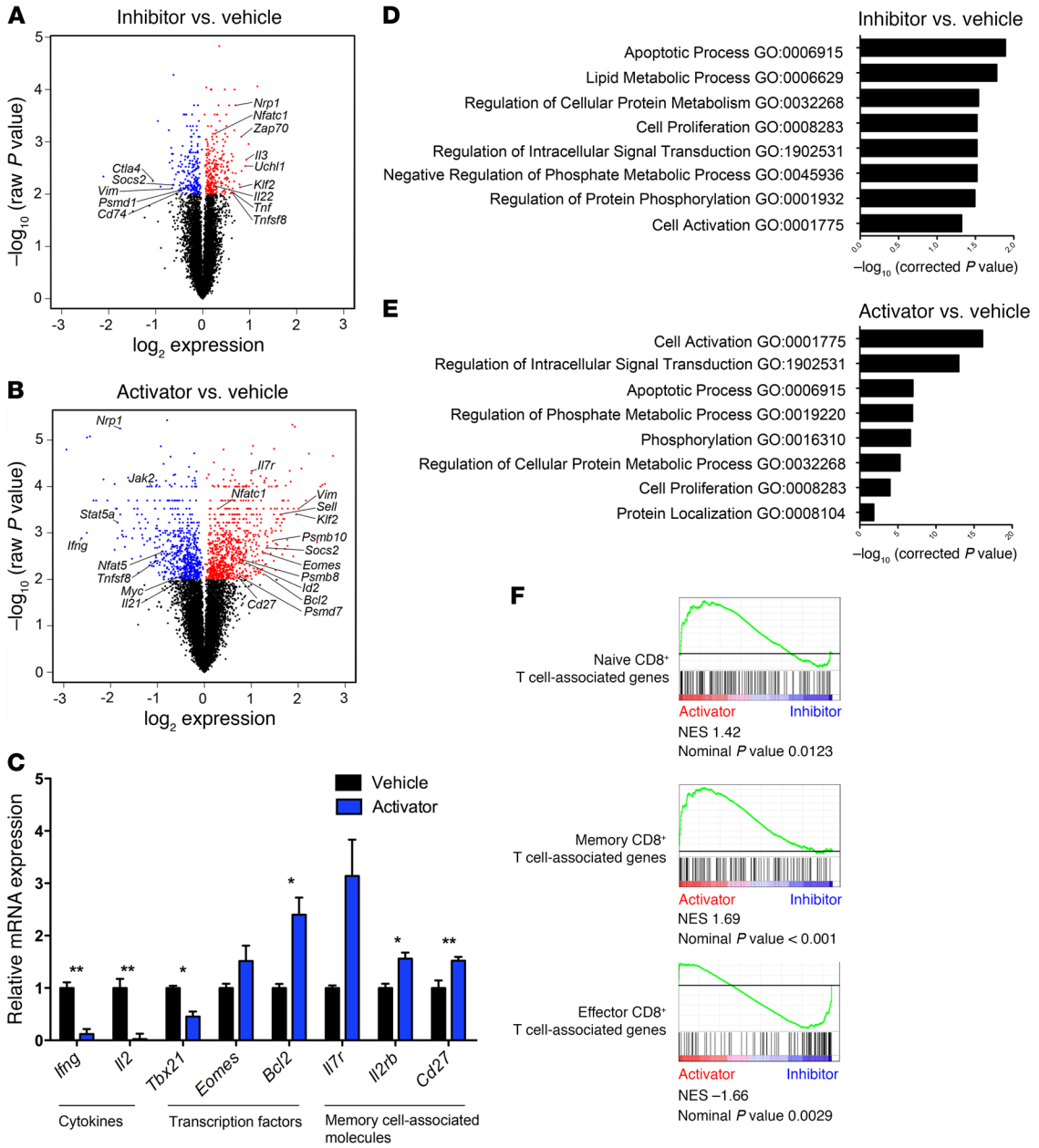

Figure 6. Modulating proteasome activity in activated CD8⁺ T cells alters their gene expression. (**A** and **B**) Volcano plots depicting differentially expressed genes derived from microarray gene expression analysis in CD8⁺ T cells treated with (**A**) proteasome inhibitor or (**B**) proteasome activator prior to activation with anti-CD3 and anti-CD28 antibodies for 24 hours, compared with gene expression of vehicle-treated cells. The *x* axis represents normalized $\log_2$ expression, and the *y* axis represents significance as $-\log_{10}$ (*t* test *P* value). Each dot represents an individual gene; red or blue represents significantly differentially upregulated or downregulated genes, respectively. (**C**) mRNA expression of selected cytokines, transcription factors, and memory-associated genes in proteasome activator–treated CD8⁺ T cells 24 hours following activation with anti-CD3 and anti-CD28 antibodies. Expression is shown relative to vehicle-treated cells and normalized to the average of *Rpl13* and *Rn18s* RNA. (**D** and **E**) Gene Ontology Biological Processes of differentially expressed gene sets are shown in order of significance as $-\log_{10}$(corrected *P* value). (**F**) GSEA of functional enrichment of differentially expressed genes in proteasome inhibitor–treated versus proteasome activator–treated cells; naive, effector, and memory enrichment datasets were obtained from MSigDB. Enrichment score is visualized in green; NES, normalized enrichment score. Microarray data are derived from 2 biological replicates. mRNA expression data are representative of 3 biologic replicates from 3 independent experiments. Error bars represent SEM of 3 replicates. N.S., $P > 0.05$; $^*P < 0.05$, $^{**}P < 0.01$ (Student's 2-tailed *t* test).

vitro for 52 hours (at least 6 cell divisions) in media that contained either "light" or "heavy" isotopes of L-lysine and L-arginine to allow metabolic incorporation of these amino acids into proteins. After cell lysis, peptides were analyzed by multidimensional liquid chromatography–mass spectrometry (LC-MS/MS proteomics), and differentially expressed proteins were compared between experimental groups. Relative to control-treated cells, 337 proteins were found at higher levels in proteasome inhibitor–treated cells, whereas 341 proteins were found at lower levels in proteasome activator–treated cells (Figure 7, A and B). Pathway analyses of differentially abundant proteins suggested that proteasome inhibition significantly affected several metabolic processes, including ribo-

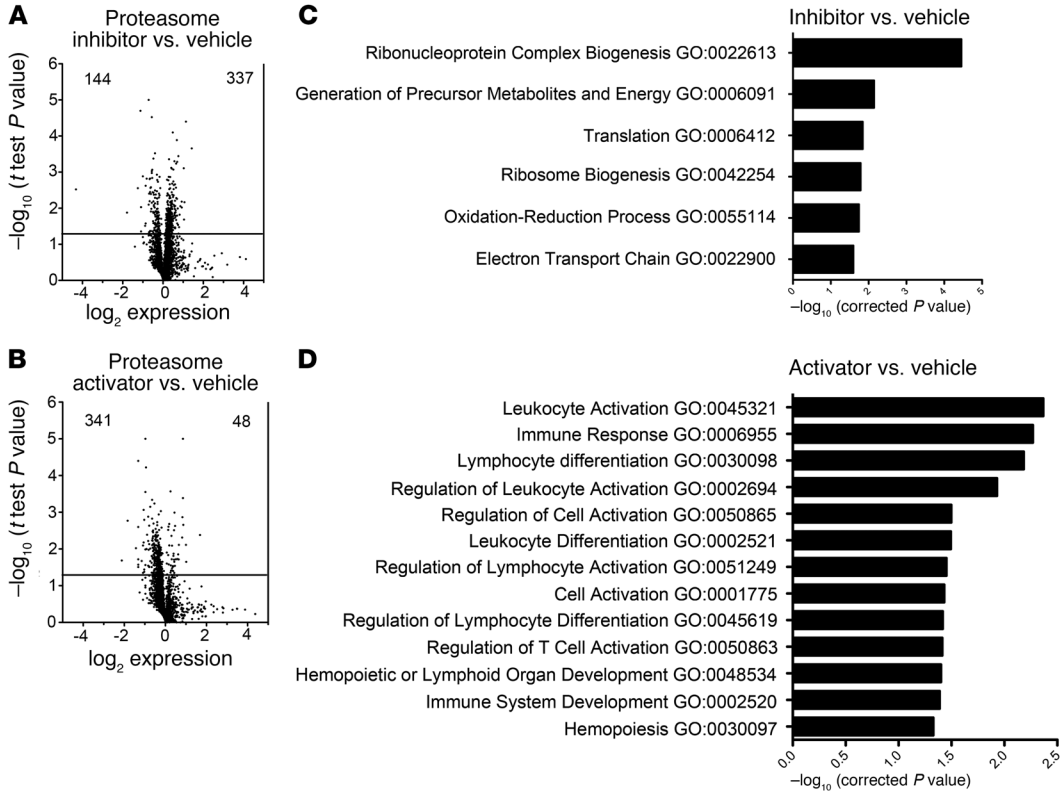

Figure 7. Modulating proteasome activity affects pathways involved in cellular metabolism. (**A** and **B**) Volcano plots depicting differentially expressed proteins derived from quantitative analysis in CD8$^+$ T cells treated with (**A**) proteasome inhibitor (**B**) or proteasome activator prior to activation with anti-CD3 and anti-CD28 antibodies for 72 hours, compared with vehicle-treated cells. Numbers in the top left and top right corners represent the number of proteins whose abundance was decreased or increased, respectively, in the proteasome-inhibited (**A**) or proteasome-activated (**B**) conditions, relative to vehicle treatment, respectively. Black horizontal line represents the threshold of significance ($P < 0.05$). (**C** and **D**) Gene Ontology Biological Processes categories enriched in proteins that were differentially expressed by proteasome inhibitor–treated (**C**) or proteasome activator–treated (**D**) cells are shown in order of significance as $-\log_{10}$(*t* test *P* value). Data are representative of 3 biologic replicates.

nucleoprotein complex biogenesis, generation of precursor metabolites, and electron transport chain activity. Proteasome activation had the most pronounced effects on pathways involving lymphocyte activation and differentiation (Figure 7, C and D). The transcriptomic analysis suggests that proteasome modulation results in differential expression of genes controlling cellular metabolism, and the findings from the proteomic screen confirm that these metabolic changes persist even after cell divisions have taken place. Taken together, these data suggest that early changes in proteasome activity can result in sustained changes in cellular metabolism that may play a role in regulating lymphocyte fate specification.

Modulating proteasome activity in CD8$^+$ T cells affects metabolic reprogramming in a Myc-dependent manner. It has been previously shown that effector T cells increase aerobic glycolysis, the process by which glucose is converted to lactate in the presence of oxygen, whereas memory T cells preferentially use oxidative phosphorylation to meet metabolic demands (38, 39). To test the possibility that differential levels of proteasome activity might exert distinct effects on metabolic reprogramming, we examined the levels of glycolysis and oxidative phosphorylation in CD8$^+$ T cells transiently treated with proteasome inhibitor, proteasome activator, or vehicle prior to activation in vitro for 72 hours. Proteasome inhibitor–treated cells exhibited an increased extracellular acidification rate (ECAR), which represents glycolytic activity, as well as glucose uptake compared with control-treated cells, while proteasome activator–treated cells exhibited decreases in these processes (Figure 8, A and B). Conversely, proteasome inhibitor–treated cells exhibited a decreased maximal respiratory capacity, while proteasome activator–treated cells exhibited an increase (Figure 8C). In support of the hypothesis that low levels of proteasome activity may promote glycolysis, we observed that inhibitor-treated cells exhibited increased expression of genes associated with glycolysis and glutaminolysis, such as *Glut1*, *Hk2*, *Eno1*, *Ldha*, and *Pfkp* (Figure 8D); by contrast, these genes did not differ in expression between control-treated and activator-treated cells (Supplemental Figure 7). Taken together, these results suggest that low levels of proteasome activity may promote metabolic reprograming by enhancing the expression of key metabolic genes involved in the glycolytic program.

We next sought to determine the mechanism by which proteasome activity influences the glycolytic transcriptional program. Several key transcription factors, including Myc, estrogen-related receptor α (ERRα), and hypoxia-inducible factor 1-α (HIF1α), have been shown to facilitate metabolic reprogramming by upregulating genes associated with the glycolytic pathway (1, 40–42). Conversely, Bcl-6 directly represses genes encoding the glycolytic pathway, while Foxo1 positively regulates genes involved in mitochondrial function and fatty acid metabolism (43, 44). Relative to control-treated cells, proteasome inhibitor–treated cells exhibited

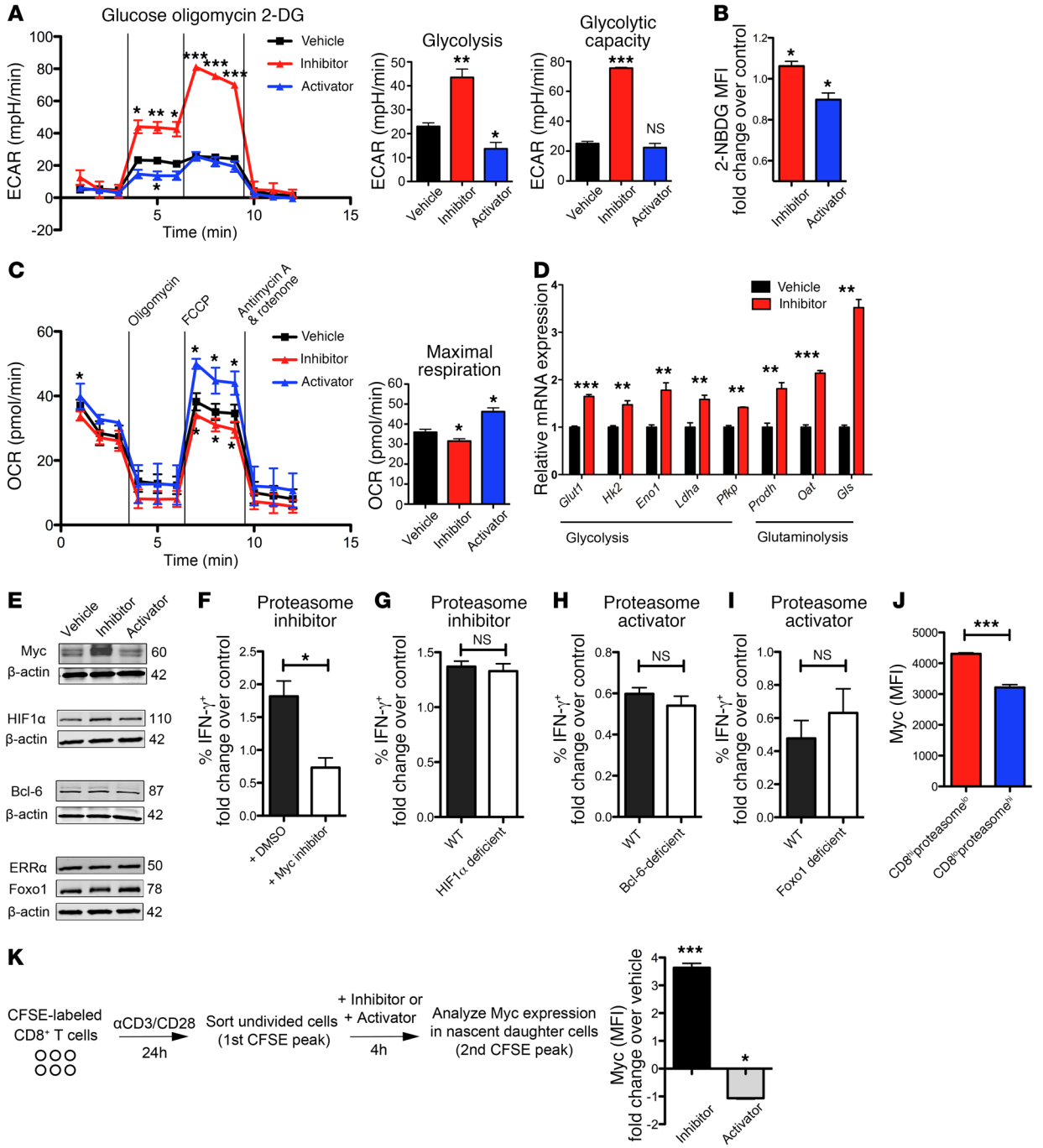

Figure 8. Proteasome activity levels in CD8⁺ T cells alters cellular metabolism in a Myc-dependent manner. (**A**) ECAR, glycolysis, or maximal glycolytic capacity of CD8⁺ T cells transiently treated with vehicle (black), proteasome inhibitor (red), or proteasome activator (blue) prior to activation for 72 hours. Compounds were added at specified time points. (**B**) Glucose uptake, as measured by 2-NBDG, in CD8⁺ T cells treated as in **A**. (**C**) OCR and maximal respiratory capacity in CD8⁺ T cells transiently treated as in **A**. Compounds were added at specified time points. (**D**) mRNA expression of genes involved in glycolysis and glutaminolysis in vehicle- or proteasome inhibitor–treated CD8⁺ T cells. Expression was normalized to *Actb*. (**E**) Immunoblot analysis of Myc, HIF1α, Bcl-6, ERRα, and Foxo1 in vehicle-, proteasome inhibitor–, and proteasome activator–treated CD8⁺ T cells. The same samples were used to probe for both ERRα and Foxo1. Molecular weights in kDa are listed. (**F**) FACS analysis of IFN-γ production in CD8⁺ T cells transiently treated with proteasome inhibitor, expressed as fold change over vehicle, followed by addition of DMSO or Myc inhibitor at 24 hours after activation. (**G**–**I**) FACS analysis of IFN-γ production, expressed as fold change over WT, in (**G**) HIF1α-deficient, (**H**) Bcl-6–deficient, or (**I**) Foxo1-deficient CD8⁺ T cells transiently treated with proteasome inhibitor. (**J**) Myc expression (MFI) in first-division proteasome activity^{lo}CD8^{hi} (red) and proteasome activity^{hi}CD8^{lo} (blue) cells. (**K**) Myc expression (MFI) in recently divided (second CFSE peak) cells arising from sorted undivided (first CFSE peak) CD8⁺ T cells treated with proteasome inhibitor or activator, relative to control-treated cells. Data are representative of 2 (**E**–**I**) or 3 independent experiments (**A**–**D**, **J**, and **K**), $n \geq 3$ replicates per group. Error bars represent SEM of 3 replicates. $^*P < 0.05$, $^{**}P < 0.01$, $^{***}P < 0.001$ (**A** and **C**, 1-way ANOVA with Dunnett's post-test; **B**, **D**, and **F**–**K**, Student's 2-tailed *t* test).

increased expression of Myc and HIF1α; however, no significant changes in the levels of ERRα, Bcl-6, or Foxo1 were observed in the setting of proteasome inhibition (Figure 8E). To confirm that proteasome activity–induced effects were not mediated through Foxo1, we also assessed nuclear translocation of Foxo1 following treatment with proteasome-modulating drugs. Although we observed a modest increase in Foxo1 nuclear translocation in cells treated with proteasome inhibitor relative to vehicle-treated cells (Supplemental Figure 8, A and B), this increase did not appear to be functionally significant, as the expression of known Foxo1 downstream targets, including TCF1 and Eomes (44, 45), was not altered.

Because we observed increased expression of Myc and HIF1α in $CD8^+$ T cells exhibiting low proteasome activity, we investigated whether these transcription factors were functionally required for the proteasome inhibitor–mediated effects on effector $CD8^+$ T cell differentiation. We assessed IFN-γ as a proxy of effector cell differentiation because its expression is dependent on the induction of glycolysis (46). We activated wild-type (WT) $CD8^+$ T cells treated with proteasome inhibitor or vehicle control and added a Myc inhibitor (47) at 24 hours following activation to avoid potential confounding effects on cell activation and proliferation (40). Strikingly, addition of Myc inhibitor prevented the increase in IFN-γ production induced by proteasome inhibition, suggesting that the proteasome-mediated effect on effector differentiation was dependent on Myc (Figure 8F and Supplemental Figure 9). By contrast, analogous experiments performed with HIF1α-deficient $CD8^+$ T cells suggested that HIF1α might be dispensable for the proteasome-mediated effects on early T cell effector differentiation (Figure 8G and Supplemental Figure 10).

Although we did not observe changes in the expression level of Bcl-6 and Foxo1 in $CD8^+$ T cells treated with proteasome inhibitor or activator, it remained possible that these molecules could nonetheless play a functional role in mediating decreased effector $CD8^+$ T cell differentiation induced by the proteasome activator. We activated Bcl-6–deficient, Foxo1-deficient, or WT $CD8^+$ T cells treated with proteasome activator or vehicle control. Bcl-6–deficient and Foxo1-deficient $CD8^+$ T cells exhibited a proteasome activator–mediated reduction in IFN-γ production comparable to that observed with control cells, suggesting that both Bcl-6 and Foxo1 may be dispensable for proteasome-mediated effects on effector differentiation (Figure 8, H and I, and Supplemental Figure 10). Taken together, these results suggest that proteasome-mediated effects on metabolic reprogramming and effector differentiation may be predominantly dependent on Myc.

Next, we sought to determine whether the Myc-dependent effects we observed were mediated through changes in mRNA, protein, or both. $CD8^+$ T cells were treated with vehicle, proteasome inhibitor, or proteasome activator; activated with anti-CD3 and anti-CD28 antibodies; then assessed at 24, 48, or 72 hours for *Myc* mRNA expression. Proteasome inhibitor–treated cells exhibited an increase in *Myc* mRNA expression compared with vehicle-treated cells, but only at 72 hours after activation (Supplemental Figure 11A). These findings suggested that changes in *Myc* at the mRNA level may be an indirect consequence of altered proteasome activity. As a complementary approach, $CD8^+$ T cells activated for 24 hours with anti-CD3 and anti-CD28 antibodies were treated with vehicle, inhibitor, or activator for 4 hours; Myc protein or mRNA was then quantitated. We added proteasome-modulating drugs to cells that had been activated for 24 hours in order to more closely model functional effects of altered proteasome activity specifically at the time of the first division, which occurs at 24 hours after activation (11). We observed that cells treated with proteasome inhibitor expressed higher levels of Myc protein, but not *Myc* mRNA (Supplemental Figure 11, B and C), suggesting that the proteasome may act predominantly by influencing the levels of Myc protein through its degradative activity. Notably, these findings do not exclude the possibility that the proteasome may also regulate *Myc* at the level of transcription, especially in light of a recent report (48) demonstrating differential expression of *Myc* mRNA by putative pre-effector and pre-memory first-division cells, which as we show (Figure 1A) exhibited distinct levels of proteasome activity.

Because antagonizing Myc has been previously shown to reduce mTORC1 signaling, we analyzed the phosphorylation state of downstream mTORC1 targets (49). mTORC1 is known to regulate cell growth, proliferation, and biosynthesis through phosphorylation of several targets, including S6 kinase and 4EBP1 (50). mTORC2 is less characterized than mTORC1 but is also known to regulate similar processes through phosphorylation of Akt and NDRG1, an upstream regulator of SGK1 (51, 52). We observed that mTORC1 targets exhibited increased phosphorylation in cells treated with proteasome inhibitor (Supplemental Figure 12A), whereas mTORC2 targets were not affected (Supplemental Figure 12B). Taken together, these findings suggest that proteasome-mediated effects on metabolism and T cell differentiation may involve the mTORC1 pathway, although it remains to be determined whether these effects are mediated through Myc.

The observation of distinct proteasome activity levels within daughter cells emerging from the first T cell division in vivo (Figure 1A), together with the finding that proteasome activity–mediated effects on effector differentiation were predominantly Myc-dependent (Figure 8, E and F), prompted us to hypothesize that Myc might also be unequally expressed in the first daughter cells by virtue of differential degradation. OT-I $CD8^+$ T cells were labeled with CFSE and adoptively transferred into recipient mice that were infected 24 hours later with Lm-OVA; splenocytes were harvested and analyzed 48 hours after infection. We observed that among cells that had undergone their first division (second CFSE peak), pre-effector cells exhibiting low proteasome activity expressed higher levels of Myc on a per-cell basis compared with pre-memory cells exhibiting high proteasome activity (Figure 8J).

We sought to link the differential levels of Myc observed in first-division pre-effector and pre-memory daughter cells with the disparate levels of proteasome activity exhibited by these cells. To experimentally model the distinct levels of proteasome activity in first-division daughter cells, we activated CFSE-labeled $CD8^+$ T cells for 24 hours in vitro and sorted the undivided parental cells (first CFSE peak) using flow cytometry. Sorted cells were then re-cultured for an additional 4 hours along with proteasome inhibitor or activator to model the low and high proteasome activity experienced by pre-effector and pre-memory daughter cells. Myc protein levels were then analyzed by flow cytometry in cells that had subsequently undergone their first division. We observed that nascent daughter cells pharmacologically induced to exhibit

low proteasome activity expressed higher levels of Myc, whereas daughter cells induced to exhibit high proteasome activity expressed lower levels of Myc (Figure 8K). Taken together, these data suggest that the low proteasome activity observed in first-division pre-effector daughter cells may result in reduced degradation and consequently increased abundance of Myc, leading to increased glycolytic activity and effector differentiation.

Discussion

While both T cell–intrinsic and –extrinsic factors have been shown to contribute to specification of $CD8^+$ T lymphocytes into terminal effector and memory cells following microbial infection (1–4), the underlying mechanisms remain incompletely understood. It has been previously demonstrated that asymmetric proteasome segregation during the first $CD8^+$ T lymphocyte division in response to microbial infection mediates unequal T-bet inheritance by the resulting daughter cells through differential degradation of T-bet protein degradation (11). However, the prior study did not directly investigate the functional consequences of asymmetric proteasome segregation on $CD8^+$ T differentiation following division. Here we show that the level of proteasome activity within a differentiating lymphocyte can play a critical role in influencing $CD8^+$ T cell fate decisions. Strikingly, differentially fated daughter cells emerging from the first division in response to microbial infection exhibit distinct levels of proteasome activity. We show that proteasome activity can be exploited pharmacologically to alter the differentiation of $CD8^+$ T cells toward the terminal effector or memory fate. Importantly, our study is the first to our knowledge to suggest that increasing proteasome activity may enhance the generation of central memory T cells. These functional consequences appear to be mediated, in part, through alterations in Myc expression that lead to metabolic reprogramming.

Regulation of endogenous proteasome activity has been previously demonstrated to play an important role in controlling cell fate decisions in multiple biologic contexts. Pluripotent stem cells exhibit higher levels of proteasome activity compared with their differentiated progeny (18, 19). Moreover, regulation of proteasome activity has been shown to influence the specification and function of cancer stem cells, a subset of cancer cells that are characterized by self-renewal capacity and the ability to initiate tumors (20, 21). Our data provide evidence supporting a role for proteasome activity in another important biologic context — $CD8^+$ T lymphocyte fate specification in response to microbial infection. We show that cells with lower proteasome activity tend to differentiate into terminal effector cells, whereas cells with high proteasome activity tend to acquire a memory cell fate. Notably, the differences in proteasome activity observed at the first division do not appear to persist as the cells continue to differentiate. This finding suggests that proteasome activity may be important in early $CD8^+$ T cell fate specification, but may no longer play the same role in "fully differentiated" terminal effector or memory cells. In support of this possibility, we recently showed that early specification versus maintenance of $CD8^+$ T cell fates may be regulated by distinct transcriptional programs (48). Using a single-cell RNA-sequencing approach, we observed that 930 genes were differentially expressed between putative pre-memory and pre-effector cells at the first division, whereas 834 genes were differentially expressed between terminal effector and memory cells. Only 115 of these transcripts were shared between these gene sets, suggesting that the majority of these differentially expressed genes may uniquely influence either early specification or maintenance of lymphocyte fate, but not both processes.

In addition to proteasome activity, other components of the ubiquitin-proteasome system have been previously shown to influence lymphocyte differentiation and function. Stability of the transcription factor Foxp3 has been shown to undergo ubiquitin-proteasome system–mediated (UPS-mediated) regulation (53, 54). Moreover, proteasome inhibition through genetic or pharmacologic approaches can attenuate experimental models of autoimmune disease by virtue of effects on antigen processing and presentation or direct effects on T lymphocytes (22–24). In another study, treatment of virally infected mice with the proteasome inhibitor bortezomib resulted in an impaired $CD8^+$ T cell response, but these effects were attributed to effects on antigen presentation due to systemic administration of the drug (55). By contrast, our data suggest that modulation of T cell–intrinsic proteasome activity can alter differentiation in response to microbial infection, with decreased proteasome activity promoting the terminal effector cell fate and increased proteasome activity promoting the central memory cell fate.

Another factor that has recently been shown to influence the differentiation of $CD8^+$ and $CD4^+$ T cells responding to microbial infection is metabolic reprogramming (38, 39). Within the first 24 hours following T cell activation, a rapid increase in glycolysis and glutamine oxidation driven by Myc-dependent metabolic reprogramming occurs, driven by the upregulation of numerous genes encoding molecules necessary for these processes (40). At later time points, additional factors, such as HIF1α, may play an important role in sustaining the glycolytic program (56). Engagement of glycolysis by activated $CD8^+$ T cells is essential for de-repression of IFN-γ mRNA, a hallmark of effector differentiation (46). Our data suggest that a key consequence of differential proteasome activity within $CD8^+$ T cells that have undergone their first division in vivo is an alteration in their expression of Myc. These findings are consistent with recent reports demonstrating asymmetric PI3K signaling, Myc expression, and mTORC1 kinase activity following $CD8^+$ T cell division (49, 57, 58). In the current study, we provide evidence supporting a role for Myc in influencing proteasome activity–mediated effects on $CD8^+$ T cell differentiation. However, Myc is unlikely to be the only mediator, as the proteasome can target many ubiquitinated proteins, including T-bet (11), that play critical roles in T cell differentiation. In support of this possibility, we provide evidence that proteasome modulation may also influence the mTORC1 pathway, consistent with recent publications demonstrating a role for mTORC1 in $CD8^+$ T cell differentiation (58, 59).

Immunologic memory is an important goal of vaccination strategies. Recent evidence has suggested the intriguing possibility that targeting cellular metabolism may be a strategy for increasing the generation and function of memory $CD8^+$ T cells. Inhibition of the mTORC1 pathway of metabolic regulation and nutrient sensing enhanced the development of central memory $CD8^+$ T lymphocytes (60). Treatment of mice with the drug metformin promoted fatty acid oxidation and oxidative phosphorylation through an AMPK-dependent mechanism, resulting in an enhanced memory $CD8^+$ T cell response (38). Conversely, inhibition of glycolysis in $CD8^+$ T cells using

2-deoxyglucose resulted in increased formation of CD8$^+$ central memory T cells (61). Taken together, these studies suggested that increasing fatty acid oxidation and oxidative phosphorylation at the expense of glycolysis has the potential to enhance the generation of immunologic memory. Our findings here suggest that increasing proteasome activity in CD8$^+$ T cells results in key changes in cellular metabolism and raise the possibility that such an approach may be a useful strategy in enhancing the generation of central memory T cells.

Methods

Mice. All mice were housed in specific pathogen–free conditions before use. WT C57BL/6, OT-I, and P14 mice were purchased from the Jackson Laboratory. *Cd4^{Cre}Hif1α$^{fl/fl}$* mice have been previously described (42). *Cd4^{Cre}Bcl6$^{fl/fl}$* mice were provided by Shane Crotty (La Jolla Institute for Allergy and Immunology, La Jolla, California, USA) and *dLck^{Cre}Foxo1$^{fl/fl}$* mice were provided by Stephen Hedrick (UCSD).

Cell culture. Single-cell suspensions were prepared from spleens and peripheral lymph nodes of C57BL/6, OT-I, or P14 mice. For in vitro memory differentiation, TCR transgenic CD8$^+$ T cells were isolated using a CD8$^+$ T Cell Isolation Kit II (Miltenyi Biotec) and then cultured for 2 days with their cognate peptide and WT T cell–depleted splenocytes. Cells were then washed and resuspended in media containing IL-2 or IL-15 (PeproTech), along with DMSO (Sigma-Aldrich), 100 nM epoxomicin (Enzo), 1 μM proteasome activator, or 1 μM tacrolimus (Sigma-Aldrich); cells were analyzed 3 or 5 days later. In pretreatment experiments, CD8$^+$ T cells were isolated with a CD8$^+$ T Cell Isolation Kit II; treated with DMSO, 0.5 μM epoxomicin, or 1 μM proteasome activator for 4 hours; washed with culture media; then cultured with immobilized anti-CD3 and anti-CD28 (Bio X Cell) antibodies and IL-2 for 3 days. In some experiments, Myc inhibitor was added 24 hours after activation at a dose of 10 μM (47).

Proteasome activity assays. Cells were incubated with 5 μM activity-based proteasome probe (21, 28) for 2 hours at 37°C, then washed and analyzed with flow cytometry. To analyze probed cells using SDS-PAGE, cells were lysed with cold lysis buffer (50 mM Tris-HCl, pH 8.5, 150 mM NaCl, 1% Triton X-100) for 30 minutes at 4°C with vortexing. 50 μg of protein was incubated with 0.5 μM of activity-based probe for 1 hour at 37°C, then resolved on a 4-20% Tris-Glycine gel (Life Technologies). Fluorescence was detected directly from the gel using a FluorChem Q (Cell Biosciences). Proteasome activity was also measured using a Proteasome-Glo Cell-Based Assay (Promega) according to the manufacturer's instructions.

Analysis of gene expression. RNA was extracted using TRIzol (Life Technologies) with GlycoBlue coprecipitant (Ambion). RNA quality and concentration were measured using a NanoDrop spectrometer (Thermo Scientific). cDNA was synthesized using a High-Capacity cDNA Reverse Transcription Kit (Applied Biosystems). Primers were designed using Primer-BLAST (62). Quantitative PCR was performed using SsoAdvanced SYBR Green Supermix (Bio-Rad) on a CFX96 qPCR machine (Bio-Rad). Relative mRNA was quantitated using the ΔΔCt method. Primers are listed in Supplemental Table 2.

Flow cytometry, cell sorting, and antibodies. Cells were stained with fluorochrome-conjugated antibodies and analyzed on an Accuri C6 or FACSCanto II (BD Biosciences). Cell sorting was done on a FACSAria II (BD Biosciences). The following antibodies were used: anti-CD8α (clone 53-6.7), anti-CD45.1 (A20), anti-CD25 (PC61), anti-CD62L (MEL-14), anti-CD44 (IM7), anti–IFN-γ (XMG1.2), anti–TNF-α (MP6-XT22), anti-KLRG1 (2F1), anti–IL-7R (A7R34), anti-CD27 (LG.7F9), anti–T-bet (4B10), anti–Bcl-2 (BCL/10C4; all from BioLegend), and anti-Gzmb (GB11, Life Technologies). Intracellular antigens were stained with a Transcription Factor Staining Buffer Set (eBioscience) according to the manufacturer's instructions. For intracellular cytokine staining, cells were stimulated for 4 hours at 37°C with 0.5 μg/ml phorbol 12-myristate 13-acetate, 5 μg/ml ionomycin (Sigma-Aldrich) in the presence of 10 μg/ml brefeldin A (Sigma-Aldrich). Cells were fixed in 4% paraformaldehyde (Electron Microscopy Services) and permeabilized with PBS (Mediatech) containing 1% FBS (Life Technologies), 1% saponin (Sigma-Aldrich), and 0.1% sodium azide (Sigma-Aldrich), followed by staining with antibodies. Analysis was performed with FlowJo software (Tree Star).

Immunoblotting and antibodies. Cells were lysed with RIPA lysis buffer (50 mM Tris pH 8.5, 150 mM NaCl, 1% Triton X-100, 0.5% sodium deoxycholate, 0.1% SDS) in the presence of Protease Inhibitor Cocktail (Sigma-Aldrich). Protein concentration was quantitated using a DC protein assay (Bio-Rad). 20 μg of protein was resolved on 4-20% Tris-Glycine gels (Life Technologies) and transferred onto nitrocellulose membranes. Membranes were probed with the following antibodies: anti-Myc (D84C12), anti–Bcl-6 (polyclonal), anti-ERRα (E1G1J), Foxo1 (C29H4; all from Cell Signaling Technology), anti-HIF1α (polyclonal, Novus Biologicals), and anti–β-actin (AC-74, Sigma-Aldrich). Fluorochrome-conjugated secondary antibodies used were anti-rabbit Alexa Fluor 680 (Life Technologies) and anti-mouse IRDye 800 (Rockland). Fluorescent signals were detected using an Odyssey imaging system (LI-COR Biosciences).

Cytotoxicity assay. OT-I CD8$^+$ T cells were pretreated with DMSO, 0.5 μM epoxomicin, or 1 μM proteasome activator for 4 hours, washed, and then cultured with OVA peptide for 3 days. Mouse splenocytes were harvested and labeled with 5 μM and 0.5 μM eFluor 670 (eBioscience) for use as target cells. One group of labeled cells was pulsed with 1 nM peptide for 1 hour, while the other group served as an unpulsed control. CD8$^+$ T cells were cocultured in various ratios with unpulsed and pulsed target cells for 4 hours. Specific killing was shown as the difference in live percentage between pulsed and unpulsed target cells, normalized to the live percentage of unpulsed target cells.

Adoptive transfer and infection. For analysis of first-division cells, OT-I CD8$^+$ T cells were labeled with CFSE, and 3×10^6 cells were transferred intravenously into recipient mice. 24 hours later, mice were infected intravenously with 5×10^3 CFU of *L. monocytogenes* expressing full-length chicken OVA (Lm-OVA). 45 hours after infection, spleens were harvested and analyzed by flow cytometry. For analysis of cells 7 and 50 days after infection, 5×10^3 congenically marked CD45.1$^+$ OT-I CD8$^+$ T cells transiently treated with proteasome inhibitor or activator were transferred into CD45.2$^+$ recipient mice that were infected 24 hours later with Lm-OVA. Blood and splenocytes were analyzed on days 7 and 50 after infection. Mice were re-challenged ≥50 days after infection with 5×10^5 CFU Lm-OVA.

Gene expression microarray. RNA was extracted using TRIzol with GlycoBlue, then processed using an RNA Clean & Concentrator Kit (Zymo Research). RNA quality was assessed using the Agilent 2100 Bioanalyzer (Agilent Technologies). Microarray analysis was performed using the Illumina Mouse WG-6 v2.0 Expression BeadChip (Illumina) following the manufacturer's instructions. Data analysis is detailed in Supplemental Methods.

SILAC metabolic labeling and mass spectrometry. Preparation and processing of isotope-labeled $CD8^+$ T cells that had been treated with proteasome inhibitor or activator are detailed in Supplemental Methods. Proteomic analysis of purified $CD8^+$ T cell lysate proteins was carried out using Multidimensional Protein Identification Technology (MudPIT) (63). Protein identification and quantitation analysis was performed as detailed in Supplemental Methods.

Cellular metabolism analysis. $CD8^+$ T cells were treated with vehicle, proteasome inhibitor, or proteasome activator for 4 hours, washed, then cultured with immobilized anti-CD3 and anti-CD28 antibodies and IL-2 for 2 days. 2×10^5 $CD8^+CD44^+$ cells were plated in triplicate and analyzed for ECAR and oxygen consumption rate (OCR) on a Seahorse XF96 (Seahorse Bioscience) according to the manufacturer's instructions. Glycolytic and mitochondrial stress tests were performed according to the manufacturer's instructions.

Statistics. An unpaired (2-tailed) Student's *t* test was used for comparisons between 2 groups. One-way ANOVA was used to measure multiple treatments compared with a control group. Repeated measures 1-way ANOVA was used for comparisons among 3 or more groups over several time points (GraphPad Prism). *P* values less than 0.05 were considered significant.

Study approval. All animal work was approved by the Institutional Animal Care and Use Committee of UCSD.

Accession codes. Gene expression array data: NCBI Gene Expression Omnibus (GEO) GSE78750. Proteomic data: MassIVE MSV000079611 (https://massive.ucsd.edu/ProteoSAFe/static/massive.jsp).

Author contributions

CEW, JGO, PJM, DAG, ATP, AWG, JDB, and JTC designed experiments. CEW, PJM, JL, SHK, and SS performed experiments and data analysis. GdB, YL, CRB, AdJ, BIF, HSO, and HO provided critical reagents and advice. JNS and JRY performed quantitative proteomics analysis. KF and ANC performed microarray analysis. CEW and JTC wrote the manuscript, and all authors contributed to manuscript editing.

Acknowledgments

We thank members of the Chang laboratory for helpful discussions and critical reading of the manuscript. This work was supported by the NIH (DK080949, OD008469, and AI095277 to JTC; P41GM103533 to JRY; AI072117 to AWG) and UCSD Digestive Diseases Research Development Center Grant DK80506; JTC is a Howard Hughes Medical Institute Physician-Scientist Early Career Awardee. CEW and PJM were supported by NIH grant T32DK007202. JNS was supported by an NIH Ruth L. Kirschstein Postdoctoral National Research Service Award (F32AG039127). DAG is a Howard Hughes Medical Institute Gilliam Fellow.

Address correspondence to: John T. Chang, 9500 Gilman Drive, Mail Code 0063, La Jolla, California 92093, USA. Phone: 858.822. 5795; Email: changj@ucsd.edu

JNS's present address is: Department of Neurology, Northwestern University Feinberg School of Medicine, Chicago, Illinois, USA

1. Chang JT, Wherry EJ, Goldrath AW. Molecular regulation of effector and memory T cell differentiation. *Nat Immunol*. 2014;15(12):1104–1115.
2. Kaech SM, Cui W. Transcriptional control of effector and memory CD8+ T cell differentiation. *Nat Rev Immunol*. 2012;12(11):749–761.
3. Kaech SM, Wherry EJ. Heterogeneity and cell-fate decisions in effector and memory CD8+ T cell differentiation during viral infection. *Immunity*. 2007;27(3):393–405.
4. Williams MA, Bevan MJ. Effector and memory CTL differentiation. *Annu Rev Immunol*. 2007;25:171–192.
5. Stemberger C, et al. A single naive CD8+ T cell precursor can develop into diverse effector and memory subsets. *Immunity*. 2007;27(6):985–997.
6. Gerlach C, et al. One naive T cell, multiple fates in CD8+ T cell differentiation. *J Exp Med*. 2010;207(6):1235–1246.
7. Plumlee CR, Sheridan BS, Cicek BB, Lefrançois L. Environmental cues dictate the fate of individual CD8+ T cells responding to infection. *Immunity*. 2013;39(2):347–356.
8. Betschinger J, Knoblich JA. Dare to be different: asymmetric cell division in Drosophila, C. elegans and vertebrates. *Curr Biol*. 2004;14(16):R674–R685.
9. Chang JT, et al. Asymmetric T lymphocyte division in the initiation of adaptive immune responses. *Science*. 2007;315(5819):1687–1691.
10. Joshi NS, et al. Inflammation directs memory precursor and short-lived effector CD8(+) T cell fates via the graded expression of T-bet transcription factor. *Immunity*. 2007;27(2):281–295.
11. Chang JT, et al. Asymmetric proteasome segregation as a mechanism for unequal partitioning of the transcription factor T-bet during T lymphocyte division. *Immunity*. 2011;34(4):492–504.
12. Kincaid EZ, et al. Mice completely lacking immunoproteasomes show major changes in antigen presentation. *Nat Immunol*. 2011;13(2):129–135.
13. Zanker D, Waithman J, Yewdell JW, Chen W. Mixed proteasomes function to increase viral peptide diversity and broaden antiviral CD8+ T cell responses. *J Immunol*. 2013;191(1):52–59.
14. Glickman MH, Ciechanover A. The ubiquitin-proteasome proteolytic pathway: destruction for the sake of construction. *Physiol Rev*. 2002;82(2):373–428.
15. Kisselev AF, Goldberg AL. Monitoring activity and inhibition of 26S proteasomes with fluorogenic peptide substrates. *Meth Enzymol*. 2005;398:364–378.
16. Peth A, Besche HC, Goldberg AL. Ubiquitinated proteins activate the proteasome by binding to Usp14/Ubp6, which causes 20S gate opening. *Mol Cell*. 2009;36(5):794–804.
17. Finley D. Recognition and processing of ubiquitin-protein conjugates by the proteasome. *Annu Rev Biochem*. 2009;78:477–513.
18. Vilchez D, et al. Increased proteasome activity in human embryonic stem cells is regulated by PSMD11. *Nature*. 2012;489(7415):304–308.
19. Jang J, Wang Y, Kim HS, Lalli MA, Kosik KS. Nrf2, a regulator of the proteasome, controls self-renewal and pluripotency in human embryonic stem cells. *Stem Cells*. 2014;32(10):2616–2625.
20. Pan J, Zhang Q, Wang Y, You M. 26S proteasome activity is down-regulated in lung cancer stem-like cells propagated in vitro. *PLoS One*. 2010;5(10):e13298.
21. Banno A, et al. Downregulation of 26S proteasome catalytic activity promotes epithelial-mesenchymal transition. *Oncotarget*. 2016;7(16):21527–21541.
22. Muchamuel T, et al. A selective inhibitor of the immunoproteasome subunit LMP7 blocks cytokine production and attenuates progression of experimental arthritis. *Nat Med*. 2009;15(7):781–787.
23. Kalim KW, Basler M, Kirk CJ, Groettrup M. Immunoproteasome subunit LMP7 deficiency and inhibition suppresses Th1 and Th17 but enhances regulatory T cell differentiation. *J Immunol*. 2012;189(8):4182–4193.
24. Basler M, Dajee M, Moll C, Groettrup M, Kirk CJ. Prevention of experimental colitis by a selective inhibitor of the immunoproteasome. *J Immunol*. 2010;185(1):634–641.
25. Yanaba K, et al. The proteasome inhibitor bortezomib inhibits T cell-dependent inflammatory responses. *J Leukoc Biol*. 2010;88(1):117–122.
26. Rasid O, Meulenbroeks C, Gröne A, Zaiss D, Sijts A. Enhanced inflammatory potential of CD4+ T-cells that lack proteasome immunosubunit expression, in a T-cell transfer-based colitis model. *PLoS One*. 2014;9(4):e95378.
27. Berkers CR, et al. Profiling proteasome activity in tissue with fluorescent probes. *Mol Pharm*. 2007;4(5):739–748.
28. Florea BI, et al. Activity-based profiling reveals reactivity of the murine thymoproteasome-specific subunit beta5t. *Chem Biol*. 2010;17(8):795–801.

29. Arsenio J, Kakaradov B, Metz PJ, Kim SH, Yeo GW, Chang JT. Early specification of CD8+ T lymphocyte fates during adaptive immunity revealed by single-cell gene-expression analyses. *Nat Immunol*. 2014;15(4):365–372.
30. Leestemaker Y, et al. Proteasome activation by small molecules. *Cell Chem Biol*. 2017;24(6):725–736.e7.
31. Manjunath N, et al. Effector differentiation is not prerequisite for generation of memory cytotoxic T lymphocytes. *J Clin Invest*. 2001;108(6):871–878.
32. Borel JF, Feurer C, Gubler HU, Stähelin H. Biological effects of cyclosporin A: a new antilymphocytic agent. *Agents Actions*. 1976;6(4):468–475.
33. Clipstone NA, Crabtree GR. Identification of calcineurin as a key signalling enzyme in T-lymphocyte activation. *Nature*. 1992;357(6380):695–697.
34. Liu J, Farmer JD, Lane WS, Friedman J, Weissman I, Schreiber SL. Calcineurin is a common target of cyclophilin-cyclosporin A and FKBP-FK506 complexes. *Cell*. 1991;66(4):807–815.
35. Huber M, Lohoff M. IRF4 at the crossroads of effector T-cell fate decision. *Eur J Immunol*. 2014;44(7):1886–1895.
36. Hendriks J, Gravestein LA, Tesselaar K, van Lier RA, Schumacher TN, Borst J. CD27 is required for generation and long-term maintenance of T cell immunity. *Nat Immunol*. 2000;1(5):433–440.
37. Grayson JM, Zajac AJ, Altman JD, Ahmed R. Cutting edge: increased expression of Bcl-2 in antigen-specific memory CD8+ T cells. *J Immunol*. 2000;164(8):3950–3954.
38. Pearce EL, et al. Enhancing CD8 T-cell memory by modulating fatty acid metabolism. *Nature*. 2009;460(7251):103–107.
39. van der Windt GJ, Pearce EL. Metabolic switching and fuel choice during T-cell differentiation and memory development. *Immunol Rev*. 2012;249(1):27–42.
40. Wang R, et al. The transcription factor Myc controls metabolic reprogramming upon T lymphocyte activation. *Immunity*. 2011;35(6):871–882.
41. Michalek RD, et al. Estrogen-related receptor-α is a metabolic regulator of effector T-cell activation and differentiation. *Proc Natl Acad Sci U S A*. 2011;108(45):18348–18353.
42. Doedens AL, et al. Hypoxia-inducible factors enhance the effector responses of CD8(+) T cells to persistent antigen. *Nat Immunol*. 2013;14(11):1173–1182.
43. Oestreich KJ, et al. Bcl-6 directly represses the gene program of the glycolysis pathway. *Nat Immunol*. 2014;15(10):957–964.
44. Tejera MM, Kim EH, Sullivan JA, Plisch EH, Suresh M. FoxO1 controls effector-to-memory transition and maintenance of functional CD8 T cell memory. *J Immunol*. 2013;191(1):187–199.
45. Hess Michelini R, Doedens AL, Goldrath AW, Hedrick SM. Differentiation of CD8 memory T cells depends on Foxo1. *J Exp Med*. 2013;210(6):1189–1200.
46. Chang CH, et al. Posttranscriptional control of T cell effector function by aerobic glycolysis. *Cell*. 2013;153(6):1239–1251.
47. Kiessling A, Sperl B, Hollis A, Eick D, Berg T. Selective inhibition of c-Myc/Max dimerization and DNA binding by small molecules. *Chem Biol*. 2006;13(7):745–751.
48. Kakaradov B, et al. Early transcriptional and epigenetic regulation of CD8(+) T cell differentiation revealed by single-cell RNA sequencing. *Nat Immunol*. 2017;18(4):422–432.
49. Verbist KC, et al. Metabolic maintenance of cell asymmetry following division in activated T lymphocytes. *Nature*. 2016;532(7599):389–393.
50. Laplante M, Sabatini DM. mTOR signaling in growth control and disease. *Cell*. 2012;149(2):274–293.
51. García-Martínez JM, Alessi DR. mTOR complex 2 (mTORC2) controls hydrophobic motif phosphorylation and activation of serum- and glucocorticoid-induced protein kinase 1 (SGK1). *Biochem J*. 2008;416(3):375–385.
52. Sarbassov DD, Guertin DA, Ali SM, Sabatini DM. Phosphorylation and regulation of Akt/PKB by the rictor-mTOR complex. *Science*. 2005;307(5712):1098–1101.
53. van Loosdregt J, et al. Stabilization of the transcription factor Foxp3 by the deubiquitinase USP7 increases Treg-cell-suppressive capacity. *Immunity*. 2013;39(2):259–271.
54. Chen Z, et al. The ubiquitin ligase Stub1 negatively modulates regulatory T cell suppressive activity by promoting degradation of the transcription factor Foxp3. *Immunity*. 2013;39(2):272–285.
55. Basler M, Lauer C, Beck U, Groettrup M. The proteasome inhibitor bortezomib enhances the susceptibility to viral infection. *J Immunol*. 2009;183(10):6145–6150.
56. Finlay DK, et al. PDK1 regulation of mTOR and hypoxia-inducible factor 1 integrate metabolism and migration of CD8+ T cells. *J Exp Med*. 2012;209(13):2441–2453.
57. Lin WH, et al. Asymmetric PI3K signaling driving developmental and regenerative cell fate bifurcation. *Cell Rep*. 2015;13(10):2203–2218.
58. Pollizzi KN, et al. Asymmetric inheritance of mTORC1 kinase activity during division dictates CD8(+) T cell differentiation. *Nat Immunol*. 2016;17(6):704–711.
59. Pollizzi KN, et al. mTORC1 and mTORC2 selectively regulate $CD8^+$ T cell differentiation. *J Clin Invest*. 2015;125(5):2090–2108.
60. Araki K, et al. mTOR regulates memory CD8 T-cell differentiation. *Nature*. 2009;460(7251):108–112.
61. Sukumar M, et al. Inhibiting glycolytic metabolism enhances CD8+ T cell memory and antitumor function. *J Clin Invest*. 2013;123(10):4479–4488.
62. Ye J, Coulouris G, Zaretskaya I, Cutcutache I, Rozen S, Madden TL. Primer-BLAST: a tool to design target-specific primers for polymerase chain reaction. *BMC Bioinformatics*. 2012;13:134.
63. Washburn MP, Wolters D, Yates JR. Large-scale analysis of the yeast proteome by multidimensional protein identification technology. *Nat Biotechnol*. 2001;19(3):242–247.